

H. Maier, R. Neu, H. Greuner, B. Böswirth, M. Balden, S. Lindig, G.F. Matthews,
M. Rasinski, P. Wienhold, A. Wiltner and JET EFDA contributors

Qualification of Tungsten Coatings on Plasma-Facing Components for JET

“This document is intended for publication in the open literature. It is made available on the understanding that it may not be further circulated and extracts or references may not be published prior to publication of the original when applicable, or without the consent of the Publications Officer, EFDA, Culham Science Centre, Abingdon, Oxon, OX14 3DB, UK.”

“Enquiries about Copyright and reproduction should be addressed to the Publications Officer, EFDA, Culham Science Centre, Abingdon, Oxon, OX14 3DB, UK.”

The contents of this preprint and all other JET EFDA Preprints and Conference Papers are available to view online free at www.iop.org/Jet. This site has full search facilities and e-mail alert options. The diagrams contained within the PDFs on this site are hyperlinked from the year 1996 onwards.

Qualification of Tungsten Coatings on Plasma-Facing Components for JET

H. Maier¹, R. Neu¹, H. Greuner¹, B. Böswirth¹, M. Balden¹, S. Lindig¹, G.F. Matthews²,
M. Rasinski^{1,3}, P. Wienhold⁴, A. Wiltner¹ and JET EFDA contributors*

JET-EFDA, Culham Science Centre, OX14 3DB, Abingdon, UK

¹*Max-Planck-Institut für Plasmaphysik, EURATOM Association, Garching, Germany*

²*EURATOM-UKAEA Fusion Association, Culham Science Centre, OX14 3DB, Abingdon, OXON, UK*

³*Faculty of Materials Science and Engineering, Warsaw University of Technology, Warsaw*

⁴*Forschungszentrum Jülich, Euratom Association, Jülich, Germany*

* See annex of F. Romanelli et al, "Overview of JET Results",
(Proc. 22nd IAEA Fusion Energy Conference, Geneva, Switzerland (2008)).

Preprint of Paper to be submitted for publication in Proceedings of the
12th International Workshop on Plasma Burning Materials and Components for Fusion Applications,
Jülich, Germany.

(11th May 2009 - 14th May 2009)

ABSTRACT.

This contribution summarised the work that has been performed to establish the industrial production of tungsten coatings on CFC for application within the ITER-like Wall Project at JET. This comprises the investigation of vacuum plasma-sprayed coatings, physical vapour deposition tungsten/rhenium multilayers, as well as coatings deposited by combined magnetron-sputtering and ion implantation. A variety of analysis tools were applied to investigate failures and oxide and carbide formation in these systems.

1. INTRODUCTION

In late 2004 it was decided to initiate the ITER-like Wall Project at JET. The purpose of this project is to operate JET with the material combination intended for ITER, i.e. beryllium in the main chamber and tungsten in the divertor [1-3]. JET will be equipped with a fully tungsten covered divertor. Tungsten is also foreseen for parts of the main chamber. All of these tungsten surfaces will be coatings on carbon tiles, which will have only slight modifications with respect to the existing MkII gas box divertor design. Only one toroidal row of tiles will be equipped with bulk tungsten [4-6].

In the MkIIA divertor configuration the selection criteria for the tile material were the thermal conductivity, the mechanical strength, as well as the thermal expansion of the tiles in toroidal direction, which led to the choice of bi-directionally reinforced Carbon Fibre Composite tiles (CFC) [7,8]. For the MkII Gas Box (GB) configuration the divertor tiles were redesigned, but kept similar to the MkII tile designs and CFC remained the tile material of choice [9].

Since a change of the tile material was not possible within the ITER-like Wall Project, the tungsten in the divertor mostly had to be implemented in the form of tungsten coatings on CFC substrates. This materials combination, however, was expected to be problematic in terms of thermomechanics, which was supported by already existing results [10]. To mitigate this risk, it was decided to test a variety of different coating deposition methods and coating thicknesses. In parallel to other dedicated European research activities for the ITER-like Wall [11], for this purpose in 2005 a coordinated research and development activity was launched [12,13]. Within this activity five Euratom associations provided 14 different types of coatings with respect to coating deposition method and coating thickness. After a thorough investigation of the coatings' properties and high heat flux performance, two types and providers were chosen. One selected coating type were vacuum plasma spray (VPS) coatings from Plansee SE, intended for the divertor, with a nominal thickness of 200 μm . For the tungsten coated main chamber tiles 10 μm thick coatings with a molybdenum interlayer deposited by Combined Magnetron Sputtering and Ion Implantation (CMSII) by the Romanian National Institute for Laser Plasma and Radiation Physics (NILPRP) were selected. Since early 2007 the establishment of industrial series production of tungsten coatings has been pursued in close cooperation with these two institutions. The paper is organised as follows:

- Section 2 describes the activities performed for upscaling the VPS process to the coating of full-sized JET divertor tiles and the result of these activities.
- Section 3 describes the results obtained and the problems encountered with the application of tungsten/rhenium multilayer coatings.

- In Section 4 qualification results on the CMSII coatings are presented and the question of carbide formation is addressed.
- Section 5 gives a brief schematic summary of the paper
- In section 6 the conclusions and an outlook are presented.

2. UPSCALING OF THE VPS COATING PROCESS

As discussed above, the original research and development phase comprised a large variety of different coating types with respect to thickness and deposition method. For reproducibility reasons each of these types was delivered on a number of small scale test tiles. This required a considerable amount of CFC material (Dunlop DMS 780) as well as resources for machining of these test tiles, both of which naturally set limits to the number and size of the test tiles. An additional consideration was the suitability of the test tile design for analysis: For keeping the tiles suitable for scanning electron microscopy without cutting samples out, their size and weight had to be limited to values below ca. 10cm in lateral dimensions and 500 g, respectively.

Nevertheless the test tiles comprised some design features of original MkII GB divertor tiles, e.g. the mounting scheme to the back plate and their total thickness. Both are important features in terms of surface temperature evolution and heat transport, since the MkII divertor tile design relies on the thermal inertia of the tiles [8]. The test tiles had dimensions of approximately 80mm×80mm×40mm and were mounted to the back plate using a similar mounting scheme as described in [7] for the MKII divertor tiles.

The drawback of the above approach is the fact that the size of the described test tiles is considerably different from full-sized JET divertor tiles. For this reason it was agreed with the VPS coatings provider that an intermediate phase of upscaling tests should be introduced. For this phase a dedicated set of larger nearly half size test tiles was designed and then machined by the actual tile supplier. These large test tiles had lateral dimensions of 172mm×142mm and contained additionally a feature of the outer vertical target tile, i. e. a convex surface curvature in one direction. The lateral dimensions correspond to the full size of the outer vertical target in one direction and to nearly half of its size in the other. A comparison of the sizes of the three types of tiles is shown in Figure 1.

The large test tiles were coated with a 200µm VPS coating and subsequently subjected to high heat flux testing in IPP's high heat flux facility GLADIS [14, 15] as well as to further analysis.

Five large test tiles were delivered to IPP. Out of these five, however, only one was rated acceptable by the supplier after visual inspection. This was due to irregularities appearing on the coatings' surfaces. Figure 2 shows this tile after high heat flux testing in GLADIS. High heat flux loading was performed using a hydrogen neutral beam with a central power density of 16.5MW/m² and a pulse duration of 0.5s, which resulted in a peak surface temperature of approximately 1200°C depending on the start temperature. The start temperature was always kept below 200°C to account for the ductile-to-brittle transition.

This combination of power density and pulse duration represents a compromise: For a given power density and short pulses the peak surface temperature scales with the square root of the pulse duration, but the energy input increases linearly with the pulse duration. The cool-down time in

between pulses depends on the total energy to be removed. For a given target value of the peak surface temperature this means, that the number of applicable pulses in a given time can be increased by operating at high power density and low pulse duration.

The photograph shown in figure 2 was taken after the tile had been loaded with 43 pulses having the above parameters. Analysis of infrared camera data shows that the damaged areas visible in the photograph were detectable much earlier as “hot spots” in the infrared images. Actually these spots developed at independent rates and must each be considered an individual failure. One hot area clearly visible in the infrared data did not develop damage visible to the bare eye before the cyclic loading programme was stopped.

Figure 3 A shows an SEM image of a metallographic cross section from such a tungsten coating. Individual pass boundaries stemming from the coating process are clearly visible. Obviously the full thickness of the VPS coating is deposited in several passes. Figure 3(b) shows an SEM backscattering image looking into one of the damaged regions from Figure 2 at an angle of 75° to the surface normal. Note that the scale bar is half a millimetre. The image shows that the coating is partially delaminated and that the delaminated part is molten (left and right foreground). Since backscattered electrons would show a strong contrast between carbon and tungsten, the image clearly shows that the bottom of the delaminated area is not carbon. Further analysis confirmed that this is tungsten. It must therefore be concluded that the delamination did not occur at the coating/substrate interface. Instead it occurred at a pass boundary.

A second tile was subjected to cyclic loading at a reduced power density, i. e. 10.5MW/m^2 , with a pulse duration of 1.0s, which resulted in a peak surface temperature around 1000°C depending on the start temperature. The coating withstood 100 pulses without delamination damage. Cyclic loading tests with a power density corresponding to Edge Localised Modes (ELMs) in JET were performed at FZ Jülich in the JUDITH facility [16]. The coatings were subjected to 0.35GW/m^2 for 1ms up to 1000 pulses. The same failure as above, namely delamination at pass boundaries was observed [17].

On the basis of the findings described in this section it was decided to stop any further efforts on VPS coatings development. This does not necessarily mean that such a development cannot be brought to a successful stage. Instead, the decision was driven mostly by the tight schedule of the project, i. e. by lack of time and resources. Continuing the development route for too long without success would have posed an additional risk.

3. TUNGSTEN/RHENIUM MULTILAYER COATINGS

It was decided to continue the cooperation with Plansee SE with thin PVD tungsten/rhenium multilayer coatings as a backup solution. Such multilayers are applied as interlayers for Plansee’s VPS coatings routinely. A tungsten/rhenium multilayer system applied as an interlayer can also be seen at the coating/substrate interface in Figure 2. These multilayer systems were also applied to the large test tiles described in section 2. Such multilayer coatings were successfully developed up to $30\mu\text{m}$ total thickness. High heat flux tests in GLADIS were performed on these coatings and resulted in some minor extent of buckling failure type delamination on a scale of the order of 100

μm (see reference [12] for a description of this failure type). At the relatively high employed power density of $16.5\text{MW}/\text{m}^2$ such delaminated buckles showed melting. The total failed surface fraction, however, was considered to be tolerable.

Upon storage in clean ambient air for several weeks, however, these coatings developed a strong discoloration from the original metallic to a brown surface. This discoloration was distributed inhomogeneously on the coatings' surfaces. By combining electron-backscatter SEM images with energy dispersive X-ray spectroscopy this inhomogeneous discoloration was shown to be caused by the local formation of an oxide surface layer. Using X-ray Photoelectron Spectroscopy (XPS) it was possible to show that the discoloration was clearly linked to the presence of rhenium oxide Re_2O_7 . Figure 4 shows XPS data from a discoloured (top) and a metallic (bottom) surface. By comparing the identified peak energies with literature and database data [18, 19] the peaks not present in the spectrum of the metallic surface can clearly be attributed to Re_2O_7 .

Since the top layer of the multilayer system originally consists of several microns of pure tungsten, the presence of rhenium oxide on the surfaces requires an explanation. By analysing witness samples a contamination of the coatings' surfaces with Re at the end of the deposition process was excluded. This raises the question how the Re was transported to the surface of the coating. As the CFC material possesses a distinct open porosity, transport along inner surfaces could be a mechanism.

Analysing literature data [20], it can be concluded that rhenium diffusion on tungsten crystal surfaces at room temperature can only be expected to span distances in the region of a fraction of a micron only. From the above discussion it must be concluded that the mechanism leading to the formation of Re_2O_7 upon long storage of the coatings in ambient air is not understood. Since Re_2O_7 is strongly hygroscopic and reacts with water to a strong acid [21], this lack of quantitative understanding must be considered as a risk to the success of the ITER-like Wall Project, as the installation of the divertor necessarily requires storage in ambient air for long periods of time. Therefore it was decided not to pursue this line of coatings qualification.

4. CMSII COATINGS WITH MO INTERLAYER

Tungsten coatings with a thickness of $10\mu\text{m}$ and with a molybdenum interlayer deposited by CMSII NILPRP Bucharest were originally selected only for the main chamber tiles to be coated with tungsten. In the light of the results described in the previous sections these coatings were also applied to full-size divertor tiles and tested in GLADIS. The results were positive in all cases. No buckling or delamination failures were observed and the only observable effect of the high heat flux tests were the well-known tensile cracks perpendicular to the in-plane fibres (see ref [12] for a description).

Based on the above results it was decided to apply this type of coating also to the divertor tiles. On the divertor target tiles, however, it must be expected that the tiles will experience longer periods of time at rather elevated temperatures. This triggers the question of carbide formation and its influence on the thermomechanical stability of the coatings. To investigate this question a coated small test tile was vacuum baked at 1350°C for 5 hours. For pure tungsten this should lead to full recrystallisation [22]. When scaled with carbon diffusion data in tungsten from ref [20], this would correspond to an exposure time of about 20 hours at a temperature of 1200°C .

The heat treated sample was high heat flux tested in GLADIS with 50 pulses at a power density of 16.5MW/m^2 and a pulse duration of 1.5s leading to a peak surface temperature of about 1400°C . This fatigue test revealed that after the heat treatment described above the coating did show delamination failures on a small scale. An example is shown in Figure 5: Unlike the buckling failure described above, the delaminations observed here hint at brittle fracture as a failure mechanism, which could be attributed to the formation of brittle carbides. To investigate this question, the sample was subsequently investigated by x-ray diffraction and by analytical electron microscopy: A cross-section was prepared by Focussed Ion Beam (FIB) preparation. An example from this is shown in Figure 6. This cross-section was analysed by energy-dispersive X-ray diffraction and by electron backscatter diffraction. Combining the information from all these investigations, the individual tungsten phases visible in Figure 6 can be identified: From top to bottom they are pure tungsten, tungsten subcarbide W_2C and tungsten carbide WC , which is consistent with the fact that the substrate as the carbon source is located at the bottom, it is not visible in the figure. From this investigation it can be concluded that combined temperature history of vacuum baking plus GLADIS testing leads to a state, where nearly all of the tungsten is converted into carbides.

5. SUMMARY

This contribution summarises the work performed since early 2007 to establish the industrial series production of tungsten coatings in close cooperation with Plansee SE and the Romanian National Institute for Laser Plasma and Radiation Physics in Bucharest.

- Upscaling of the VPS process from the original small scale test tiles to full-size divertor tiles failed; a further improvement was not attempted due to time constraints.
- Trying to establish PVD W/Re multilayers instead was stopped due to the formation of Re_2O_7 on the coatings surface after storage in ambient air for several weeks. An unclarified Re transport mechanism is involved.
- The application of CMSII coatings with a Mo interlayer to full-size divertor tiles yielded positive test results. Carbide formation can, however, lead to small scale delaminations.

CONCLUSION AND OUTLOOK

The ITER-like Wall Project started out with a very tight schedule. In addition the available machine time for high heat flux testing and consequently the information which can be obtained from such tests are limited. For this reason not all of the decision processes mentioned in this contribution can be based on a sound scientific understanding of the observed facts. For instance the termination of a further development of vacuum plasma sprayed coatings on CFC does not necessarily mean that such a development cannot be brought to a positive result.

As all of the tungsten coatings are produced by one of the two originally selected suppliers, in retrospective the decision taken in 2006 to rely on two suppliers can be regarded as very appropriate for the boundary conditions of this project, since naturally coatings from both were investigated in parallel during the industrialisation phase of the project. Therefore one supplier can act as a backup for the other without need for additional resources for fallback options.

The results presented in section 4 indicate that in order to provide the coating lifetime required to meet the scientific goals it will be necessary to monitor and limit the total integrated time the coatings spend at elevated temperatures during the operational phase of the ITER-like Wall. Therefore a more detailed assessment of the time evolution of the carbide formation process is planned to be performed by electron microscopy and focussed ion beam preparation of cross-sections. Additionally a direct identification of all phases present in the partially carbidised coating will be performed by transmission electron microscopy.

ACKNOWLEDGEMENT

The valuable contributions of K. Bald-Soliman are acknowledged. This work was supported by the European Fusion Development Agreement.

REFERENCES

- [1]. G. Piazza et al. 2007 Journal Nuclear Materials **367-370** 1438
- [2]. J. Pamela et al. 2007 Journal Nuclear Materials **363-365** 1
- [3]. G. F. Matthews et al. 2007 Phys. Scr **T128** 137
- [4]. T. Hirai et al. 2007 Fus. Eng. Des. **82** 1839
- [5]. Ph. Mertens et al. 2009 Fus. Eng. Des. doi:10.1016/j.fusengdes.2008.11.055 in press
- [6]. Ph. Mertens et al. these proceedings
- [7]. H. Altmann et al. 1994 Proc. 18th SOFT Fusion Techn. **1994** 275
- [8]. M. Pick et al. 1995 Journal Nuclear Materials **220-222** 595
- [9]. H. Altmann et al. 1997 Proc. 19th SOFT Fusion Techn. **1996** 483
- [10]. H. Maier 2005 Mater. Sci. Forum **475-479** 1377
- [11]. H. Maier et al. 2007 Nuclear Fusion **47** 222
- [12]. H. Maier et al. 2007 Journal Nuclear Materials **363-365** 1246
- [13]. R. Neu et al. 2007 Phys. Scr. **T128** (2007) 150
- [14]. H. Greuner et al. 2005 Fusion Engineering Design **75 (9)** 333
- [15]. H. Greuner et al. 2007 Journal Nuclear Materials **367-370** 1444
- [16]. R. Duwe, W. Kühnlein, M. Münstermann, 1994 Proc. SOFT 1994, Fus. Technol. (1995) 335.
- [17]. T. Hirai et al. 2009 Journal Nuclear Materials doi:10.1016/j.jnucmat.2009.03.060. in press
- [18]. J. Luthin, Ch. Linsmeier 2001 Journal Nuclear Materials **290-293** 121
- [19]. NIST X-ray Photoelectron Spectroscopy Database Version 3.5 (www.nist.gov)
- [20]. O. Madelung (ed.) 1990 Landolt-Börnstein New Series III/26 (Berlin: Springer)
- [21]. E. Wiberg (ed.) 1976 Hollemann-Wiberg – Lehrbuch der anorganischen Chemie (Berlin: de Gruyter)
- [22]. W. Espe 1959 Werkstoffkunde der Hochvakuumtechnik (Berlin: VEB Deutscher Verlag der Wissenschaften)

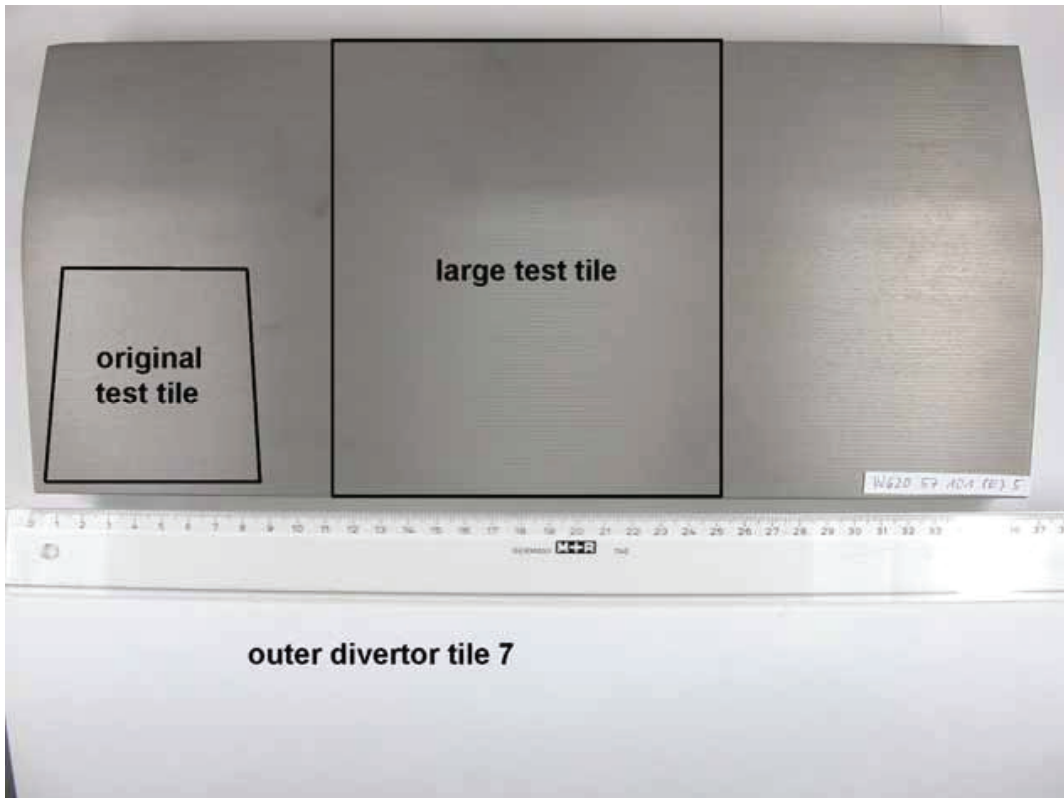


Figure 1: Outer divertor vertical target tile with the sizes of original and larger test tiles for comparison. The scale is in cm.



Figure 2: VPS coated large test tile after high heat flux loading in GLADIS for 43 pulses at 16.5MW/m^2 and a pulse duration of 0.5s. The scale is in cm

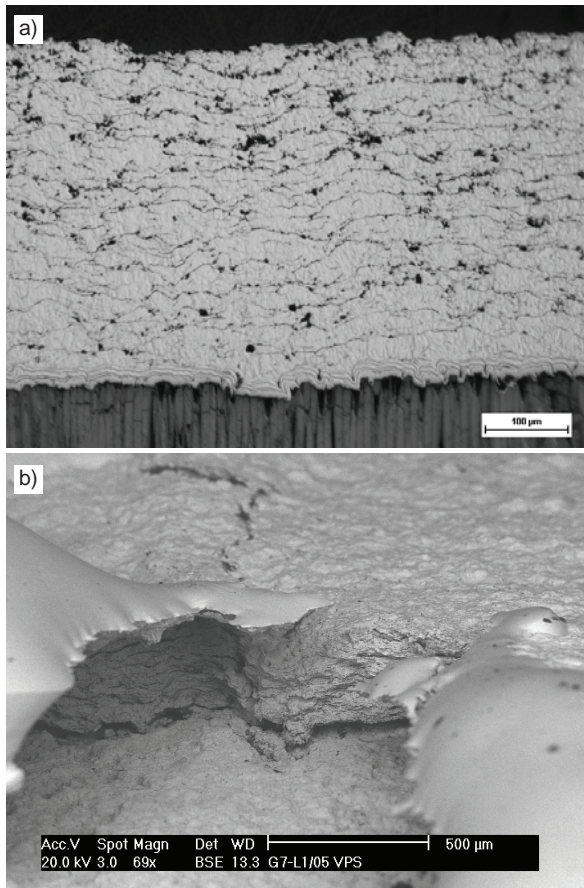


Figure 3: A) Metallographic cross-section of a VPS cross-section with visible pass boundaries, which occur due to the VPS deposition process. B) SEM image of one of the failures in Figure 1 showing that the failures occurred at pass boundaries.

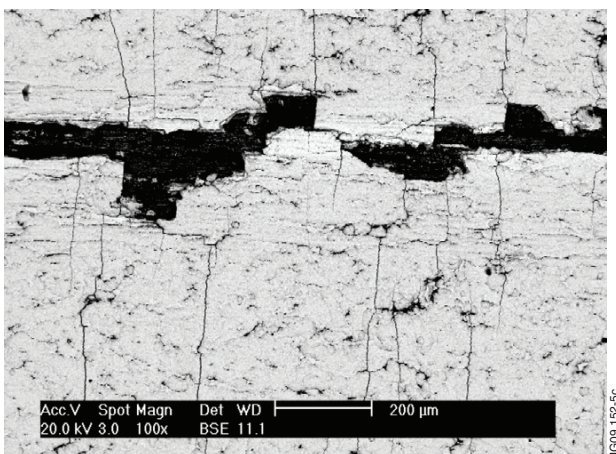


Figure 5: Backscattering electron SEM image of a CMSII coating after high heat flux testing in GLADIS showing tungsten tensile cracks (vertical lines) and small-scale delamination failure.

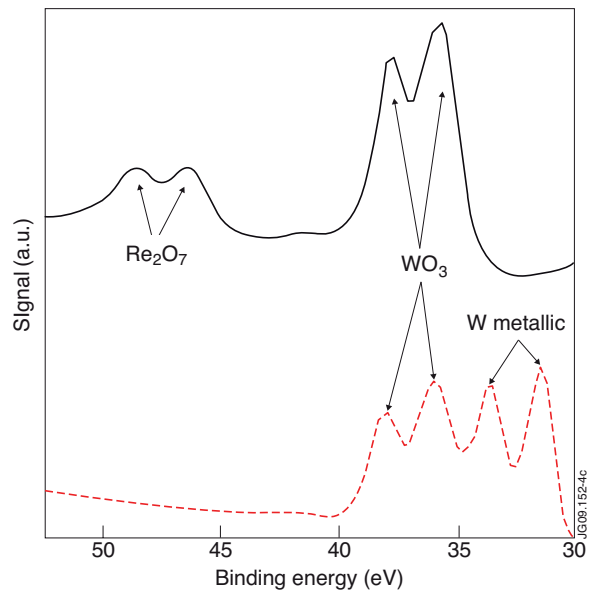


Figure 4: X-ray photoelectron spectra of original metallic (bottom) and discoloured (top) surfaces. The attributed chemical compounds are labelled.

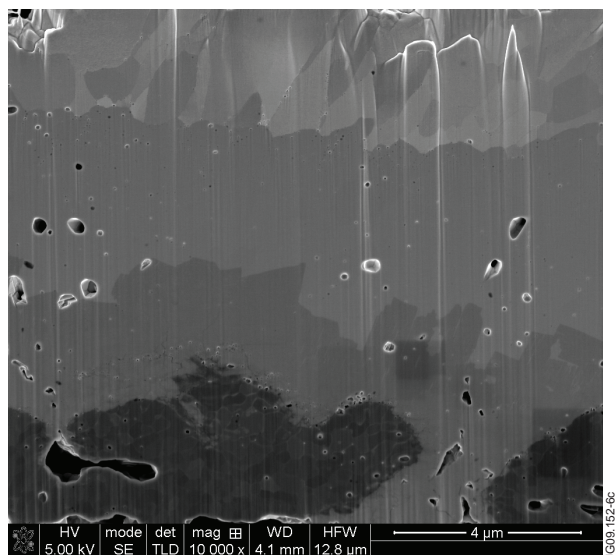


Figure 6: FIB cross section of a heat treated CMSII coating. The image shows from top to bottom: Tungsten, tungsten subcarbide W_2C , and tungsten carbide WC . The dark phase at the bottom originates from the Mo interlayer.